The Journal of Immunology

Hypochlorous Acid: A Natural Adjuvant That Facilitates Antigen Processing, Cross-Priming, and the Induction of Adaptive Immunity

Zofia M. Prokopowicz, Frederick Arce, Rafal Biedron, Cheryl L.-L. Chiang, Marta Ciszek, David R. Katz, Maria Nowakowska, Szczepan Zapotoczny, Janusz Marcinkiewicz and Benjamin M. Chain

J Immunol 2010; 184:824-835; Prepublished online 16 December 2009;
doi: 10.4049/jimmunol.0902606
http://www.jimmunol.org/content/184/2/824

The Journal of Immunology is published twice each month by
The American Association of Immunologists, Inc.,
1451 Rockville Pike, Suite 650, Rockville, MD 20852

Print ISSN: 0022-1767 Online ISSN: 1550-6606.

Hypochlorous Acid: A Natural Adjuvant That Facilitates Antigen Processing, Cross-Priming, and the Induction of Adaptive Immunity

Zofia M. Prokopowicz,* Frederick Arce,* Rafał Biedroń,† Cheryl L.-L. Chiang,* Marta Ciszek,† David R. Katz,* Maria Nowakowska,‡ Szczepan Zapotoczny,† Janusz Marcinkiewicz,† and Benjamin M. Chain*

The production of hypochlorous acid (HOCl) is a characteristic of granulocyte activation, a hallmark of the early phase of innate immune responses. In this study, we show that, in addition to its well-established role as a microbicide, HOCl can act as a natural adjuvant of adaptive immunity. HOCl enhances the T cell responses to the model Ag OVA, facilitating the processing and presentation of this protein via the class II MHC pathway. HOCl modification also enhances cross-presentation of the tumor Ag tyrosinase-related protein 2 via class I MHC. The adjuvant effects of HOCl are independent of TLR signaling. The enhanced presentation of HOCl-modified OVA is mediated via modification of the N-linked carbohydrate side chain rather than formation of protein aldehydes or chloramines. HOCl-modified OVA is taken up more efficiently by APCs and is degraded more efficiently by proteinases. Atomic force microscopy demonstrated that enhanced uptake is mediated via specific receptor binding, one candidate for which is the scavenger receptor lectin-like oxidized low-density lipoprotein receptor, which shows enhanced binding to chlorinated OVA. A function of HOCl is therefore to target glycoprotein Ags to scavenger receptors on the APC surface. This additional mechanism linking innate and adaptive immunity suggests novel strategies to enhance immunity to vaccines. ***The Journal of Immunology*****, 2010, 184: 824–835.**

Innate immunity regulates the induction of adaptive immune responses via multiple interactions. The paradigm is based on the regulation of APC maturation and migration via ligation of pattern recognition receptors, but other examples include the ability of complement fragments to enhance B cell activation via CD21 (1) or direct effects of TLR ligation on lymphocyte activation (2). Typically, an innate immune response precedes and is necessary for strong and persistent adaptive immunity. In the absence of innate immunity, most Ags stimulate a weak and transient adaptive immune response, and this may result in tolerance rather than protection. Recent studies also suggest that many classical adjuvants work by promoting the innate/adaptive axis (3). A more complete understanding of the complex interaction between these two components is therefore a key to understanding and manipulating the vertebrate immune response.

Dendritic cells (DCs) play a pivotal role in facilitating the interaction between innate and adaptive immunity. DC uptake (4), processing (5), and loading of Ag onto MHC molecules, transport of Ag via migration from tissues to local lymph nodes or spleen (6), and finally presentation and costimulation of T cells all can be regulated by signals from innate immunity. Although earlier studies of innate immune regulation focused primarily on the regulation of migration and costimulation, more recent studies have focused on the earlier stages of uptake, processing, and MHC loading. DC maturation is accompanied by a complex sequence of changes in the Ag processing machinery (7), and recent studies have suggested that TLR signaling in DCs may be a prerequisite for efficient Ag loading (8). The response of the DCs to inflammatory cytokines can result in qualitative as well as quantitative changes in Ag processing, determining both the strength and the repertoire of the ensuing adaptive immune response (9).

There are several mechanisms by which innate immunity regulates DC Ag processing. At the site of infection, DCs are activated directly by ligation of their pattern recognition receptors by pathogen associated molecular patterns as well as by a variety of pro- and anti-inflammatory chemokines and cytokines. However, because activated neutrophils are recruited rapidly to most inflammatory sites, they are a likely component of the DC microenvironment early in immune activation. A major protein constituent of the neutrophil, found in the primary azurophil granules, is myeloperoxidase, an enzyme that catalyses the conversion of hydrogen peroxide to hypochlorous acid (HOCl) and to a lesser extent to hypobromous acid (10). These unstable strong oxidants were believed previously to act predominantly as bactericidal agents within the phagolysosome, but there is now extensive evidence that the enzyme and its products also act

*Division of Infection and Immunity, University College London, London, United Kingdom; †Department of Immunology, Jagiellonian University Medical College; and ‡Department of Physical Chemistry and Electrochemistry, Faculty of Chemistry, Jagiellonian University, Kraków, Poland

Received for publication August 10, 2009. Accepted for publication November 16, 2009.

This work was supported by the following: Atomic force microscopy experiments were supported by the Foundation for Polish Science Team Programme and cofinanced by the European Union European Regional Development Fund, PolyMed, TEAM/2008-2/6; Z.M.P. was supported by a Medical Research Council studentship; M.C. and J.M. were supported by Jagiellonian University Medical College Grant K/ZDS/001008; and B.M.C. was supported by a grant from the Biotechnology and Biological Sciences Research Council Selective Chemical Intervention in Biological Systems initiative.

Address correspondence and reprint requests to Prof. Benjamin M. Chain, Division of Infection and Immunity, Windeyer Building, University College London, 46 Cleveland Street, London W1T4JP, U.K. E-mail address: B.chain@ucl.ac.uk

The online version of this article contains supplemental material.

Abbreviations used in this paper: AFM, atomic force microscopy; DC, dendritic cell; HEL, hen egg lysozyme; HOCl, hypochlorous acid; Lox-1, lectin-like oxidized low-density lipoprotein receptor; TRIF, Toll/IL-1R domain-containing adaptor-inducing IFN-β; TRITC, tetramethylrhodamine isothiocyanate; Trp2, tyrosinase-related protein 2.

www.jimmunol.org/cgi/doi/10.4049/jimmunol.0902606

extracellularly, resulting in very specific oxidative modifications to lipids (11), enzymes (12), and extracellular matrix (13), all of which are components in the inflammatory microenvironment. Chlorinated lipids have been shown previously to induce DC maturation (14).

In this study, we identify a mechanism whereby protein chlorination targets glycoproteins to scavenger receptors on the APC, promoting Ag uptake and processing by APCs such as DCs. Therefore, we propose that in an inflammatory/immune milieu HOCl derived from neutrophils may represent a natural innate immune-derived adjuvant that can promote induction of adaptive immunity.

Materials and Methods

Animals

Six- to 8-wk-old C57BL/6 and BALB/c mice were obtained from Harlan (Bicester, U.K.) and maintained by Biological Services, University College London, London, U.K. Spleen cells from TCR transgenic mice expressing the OTII anti-OVA receptor were a kind gift from Prof. M. Collins (University College London, London, U.K.). Toll/IL-1R domain-containing adaptor-inducing IFN-β (TRIF)/MyD88 double-knockout mice were obtained from Cancer Research UK (London, U.K.). All of these experiments were carried out under U.K. Animal Project License authorization. In vivo Ab responses were determine using 8- to 10-wk-old BALB/c female mice housed at the Department of Immunology, Jagiellonian University Medical College, Kraków, Poland. The experimental procedures used were approved by the local Jagiellonian University Ethical Committee on Animal Experiments.

Protein chlorination

OVA (grade V; Sigma-Aldrich, Poole, U.K.) (2 mg/ml), endotoxin-free OVA (Endograd, Profos, Germany) (2 mg/ml), or hen egg lysozyme (HEL) (Boehringer Mannheim, Mannheim, Germany) (0.5–2 mg/ml) was dissolved in HBSS and mixed with NaOCl (Sigma-Aldrich) at various molar ratios. The reaction was incubated at 37˚C for 1 h. The NaOCl concentration was determined before each reaction by absorbance measurements at 292 nm using a molar extinction coefficient of 350 M^{-1} cm^{-1}. The modified protein was purified and transferred into cell culture medium by passage over a PD-10 Sephadex G-25 column (GE Healthcare, Chalfont, U.K.) according to the manufacturer's instructions. In some experiments, the chlorinated protein was reduced by addition of 50 mM $NaBH_4$ (Sigma-Aldrich) and further incubation for 1 h at 37˚C. Alternatively, protein chloramines were converted back to free amines by addition of 30 mM L-methionine (Sigma-Aldrich) and incubation for 30 min at room temperature. Samples were stored in −20˚C. Carbonyl groups were quantified by reaction with 2,4-DNP-hydrazine (Camlab, Cambridge, U. K.) (15). Amino groups were quantified by reaction with 2,4,6-trinitrobenzenesulfonic acid (Fluka, Sigma-Aldrich).

Preparation of bead-conjugated Ags

OVA and OVA_{Cl}^{I} were adsorbed onto fluorescent beads (1-μm sulfate microspheres, red fluorescent 580/605, Molecular Probes/Invitrogen, Eugene, OR) according to the manufacturer's instructions. Presence of the protein on the beads was confirmed by Western blot analysis.

B16.F10 melanoma cells

The C57BL/6-derived mouse melanoma B16, subline F10, which expresses tyrosinase-related protein 2 (Trp2) was a kind gift from Dr. Jonathan Silk (Tumor Immunology Unit, Weatherall Institute of Molecular Medicine, John Radcliffe Hospital, Oxford, U.K.) and was cultured in complete RPMI 1640 medium at 37˚C and 5% CO_2.

B16.F10 melanoma cells (8×10^5 cells per milliliter) were incubated in the presence of HOCl (60 μM) in HBSS for 1 h at 37˚C and excess HOCl removed by washing twice with HBSS. In some experiments, B16.F10 cells were incubated in HBSS at 56˚C for 30 min and then washed twice with HBSS. Both procedures induced 100% cell death as measured by propidium iodide or trypan blue staining.

Vaccination of mice with DCs pulsed with chlorinated B16.F10 melanoma cells

Bone marrow DCs were cocultured with B16.F10 cells (chlorinated or heat-killed) at a ratio of 1:1 or with medium alone for 24 h at 37˚C and 5% CO_2. The DCs were harvested, washed twice, and resuspended in HBSS. Each C57BL/6 mouse was injected in the tail vein with DCs (10^6 cells per mouse). Two weeks after injection, the mice were sacrificed, and the spleen cells were cultured with chlorinated B16.F10 (at a ratio of 1 tumor cell to 10 spleen cells) or medium without Ag for a further week in vitro. Viable splenocytes (>80% T cells, 10^6 cells per well) were evaluated for IFN-γ ELISpot (Millipore, Bedford, MA) responses against chlorinated B16.F10 cells (10^5 cells) or a peptide coding the major Trp2 CD8 epitope (1 μM) or medium alone.

Peptides

The synthetic peptides coding for OVA 323–339 (ISQAVHAAHAEINEAGR) recognized by DO11.10 T cells and OTII cells, OVA 273–288 (MEERKIKVYLPRMKME) recognized by 3DO18.3 T cells, OVA 257–278 (SIINFEKLTEWTSSNVMEERKI) recognized by MF2.D9 T cells, and Trp2 (SVYDFFVWL) were synthesized and purified by the Cancer Research UK peptide synthesis facility.

DCs and macrophage culture

Bone marrow cells were isolated from hind leg femurs and tibias of one mouse, and a single-cell suspension of bone marrow cells was plated in a six-well plate. The bone marrow cells were cultured in IMDM (Invitrogen) supplemented with 10% FCS (PAA Laboratories, Haidmannwerg, Austria), 5×10^{-5} M 2-ME (Life Technologies, Paisley, U.K.), 100 U/ml penicillin/streptomycin (Sigma-Aldrich), and 20 ng/ml rGM-CSF (PeproTech, Rocky Hill, NJ). On day 4, the rGM-CSF was renewed. On day 7 of culture, cells were harvested and purified by positive selection using magnetic $CD11c^+$ beads according to the manufacturer's instructions (MicroBeads; Miltenyi Biotec, Auburn, CA).

Bone marrow-derived macrophages were cultured in DMEM supplemented with 10% FCS, 100 U/ml penicillin/streptomycin, and 10% supernatant from L929 cells, which was changed on day 3 of culture. On day 6, media was replaced with fresh DMEM supplemented with 10 ng/ml IFN-γ (PeproTech). After 2 d of culture, cells were harvested and used immediately.

Splenic DCs

Fresh spleens were obtained from mice injected previously with FITC-OVA, FITC-OVA_{Cl}^{I}, or HBSS and diced. Spleen fragments were incubated in collagenase type II (200 μg/ml; Sigma-Aldrich) and DNase I (500 μg/ml; Sigma-Aldrich) for 30 min at room temperature. Collagenase activity was stopped with EDTA (10 mM, 5 min; Sigma-Aldrich). The single-cell suspension was treated with RBC lysis buffer (Hybri-Max; Sigma-Aldrich) for 3 min at room temperature, washed twice with HBSS, and purified by positive selection using magnetic $CD11c^+$ beads according to the manufacturer's instructions (MicroBeads; Miltenyi Biotec).

T cells

OVA-specific T cell hybridomas DO11.10, 3DO18.3, and MF2.2D9 (kind gift from Dr. K. Rock, University of Massachusetts, Worcester, MA) were cultured in DMEM supplemented with 10% FCS and 100 U/ml penicillin/streptomycin. The HEL T cell hybridoma Ad71–85 (kind gift from Dr. Eli Sercarz, University of California, Los Angeles, Los Angeles, CA) was cultured in RPMI 1640 supplemented with 10% FCS, 100 U/ml penicillin/streptomycin, and 5×10^{-5} M 2-ME. CTLL-2 indicator cells were cultured in IMDM supplemented with 10% FCS, 100 U/ml penicillin/streptomycin, 5×10^{-5} M 2-ME, and 10 ng/ml IL-2 (PeproTech). OTII cells were cultured from spleens of mice expressing the OTII TCR (16). Single-cell suspensions of spleen cells were cultured for 24 h in RPMI 1640 supplemented with 10% FCS, 100 U/ml penicillin/streptomycin, 5×10^{-5} M 2-ME, and 250 nM OVA 323–339 peptide and then expanded for 6 d in complete RPMI 1640 supplemented with 10 ng/ml IL-2. The cells were stored at −80˚C until required. Before stimulation, cells were thawed rapidly and washed, then used immediately.

Ag presentation assays

OVA-specific T cell hybridomas (2×10^4 cells per well) or HEL-specific hybridomas (5×10^4 cells per well) were cultured with purified DCs (5×10^3 or 10^4 cells per well) or with macrophages (10^4 cells per well) in the presence of Ag at the indicated concentrations. For some experiments, DCs (10^5 cells) were precultured with Ag in polypropylene tubes for different times. The excess Ag was removed by washing twice in HBSS, and the DCs were fixed with 0.05% glutaraldehyde (Sigma-Aldrich) for 30 s. Excess glutaraldehyde was removed by two more washes, and different numbers of fixed DCs were cocultured with T cell hybridomas (2×10^4 cells per well). After 24 h, the supernatants were harvested and frozen at −20˚C. IL-2 in the supernatants was measured using the IL-2–sensitive CTLL-2 indicator cells as described (17). TCR transgenic T cells (2×10^4 OT-II cells per well), expanded as described above, were cultured with purified DCs (5×10^3 cells per well) in the presence of the Ag at the indicated concentrations. For some experiments, Ag was preincubated for 30 min at room temperature with 1 μg/ml polymyxin B (Invitrogen). Thymidine incorporation was measured after 18 h as described (18).

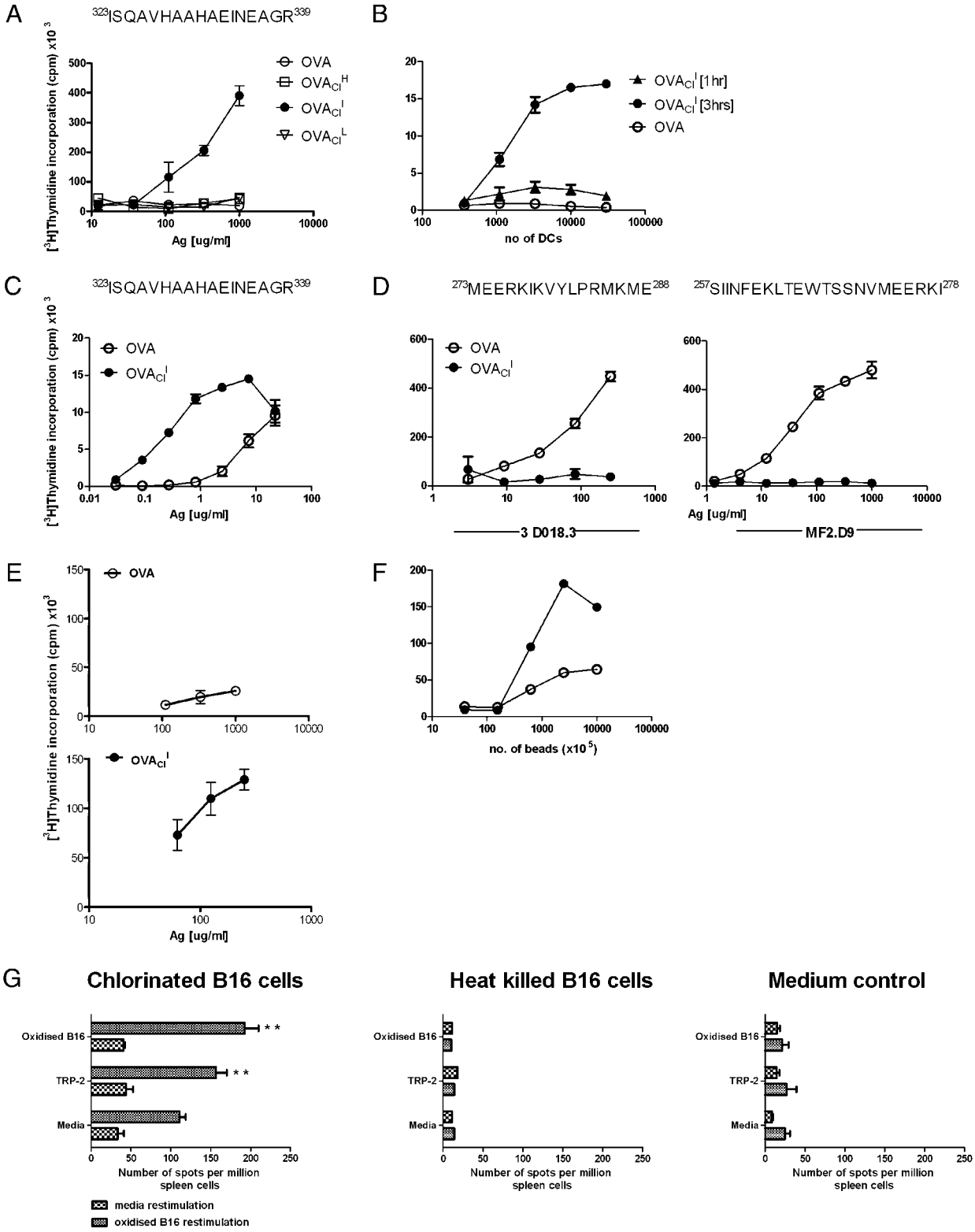

FIGURE 1. Modification with HOCl enhances the processing of OVA in vitro in an epitope-selective manner. *A*, DO11.10 hybridoma cells (which recognize the epitope sequence shown above the graph) were incubated with different concentrations of OVA or chlorinated OVA and bone marrow-derived DCs as described in *Materials and Methods*. The graph shows IL-2 release measured as thymidine incorporation of the CTLL-2 indicator cell line. *B*, OVA_{Cl}^{I} (250 μg/ml) was incubated with DCs for 1 or 3 h. Excess Ag was removed, and the DCs were fixed with glutaraldehyde, washed, and cocultured with DO11.10 hybridoma cells as in *A*. The graph shows IL-2 release measured as thymidine incorporation of the CTLL-2 indicator cell line. *C*, TCR transgenic OTII T cells were incubated with different concentrations of OVA or OVA_{Cl}^{I} and bone marrow-derived DCs as described in *Materials and Methods*. The graph shows OTII proliferation measured as thymidine incorporation. *D*, As for *A*, but using two other T cell hybridomas specific for different epitopes of OVA. *E*, DO11.10 hybridoma cells were incubated with different concentrations of OVA or OVA_{Cl}^{I} and bone marrow-derived macrophages as described in *Materials and Methods*. The graph shows IL-2 release measured as thymidine incorporation of the CTLL-2 indicator cell line. *F*, As for *E*, but using OVA or OVA_{Cl}^{I} adsorbed to 1-μm beads. Results are presented as the average ± SD [^{3}H]thymidine incorporation of triplicate cultures. Experiments were repeated twice (*B*, *E*, *F*), three times (*A*, *D*), or more (*C*). *G*, Bone marrow-derived DCs were cocultured with chlorinated B16 melanoma cells,

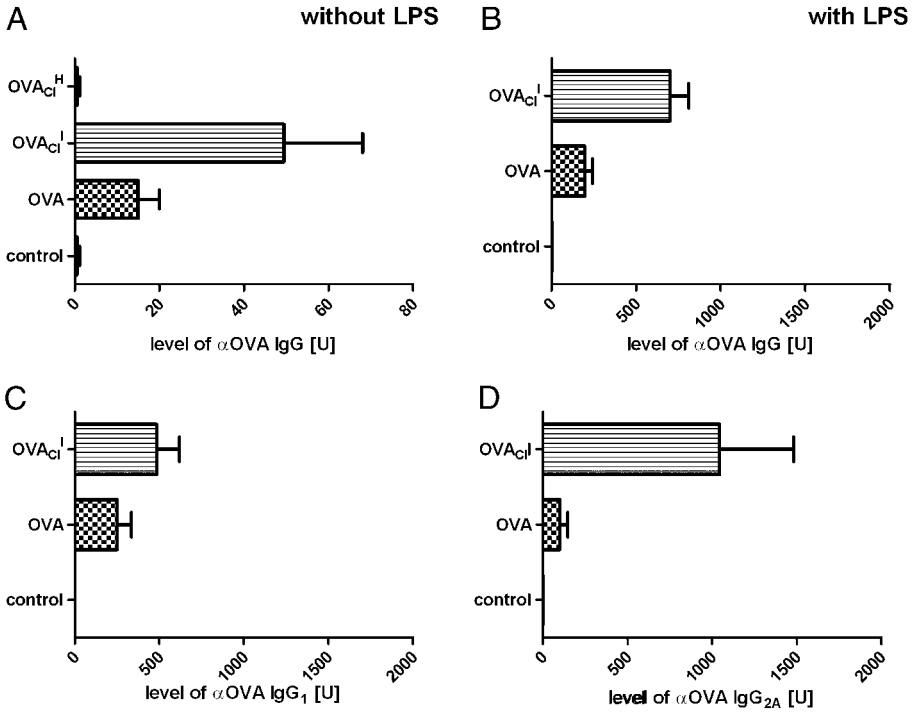

FIGURE 2. Modification with HOCl enhances the anti-OVA Ab response in vivo. Groups of five mice (BALB/c) were immunized i.p. with OVA or OVA$_{Cl}^{I}$ (200 μg) either alone (*A*) or with LPS (*B–D*) (1 μg per mouse) (primary immunization). On day 14, all of the mice were boosted with 100 μg of OVA and 1 μg of LPS. After an additional 5–7 d, mice were sacrificed, and sera were tested by ELISA for specific IgG anti-native OVA Abs. *A* and *B* show total IgG titers, whereas *C* and *D* show IgG1 and IgG2a isotype responses, respectively. All of the graphs are in arbitrary units in comparison with a standard anti-OVA Ig reference sample. *p* values for unmodified OVA versus OVA$_{Cl}^{I}$: *A*, $p < 0.08$; *B*, $p < 0.002$; *C*, $p < 0.17$; *D*, $p < 0.04$ (Student *t* test, $n = 5$).

In vivo Ab responses

Mice were immunized with OVA or OVA$_{Cl}^{I}$ (200 μg, LPS-free; Sigma-Aldrich) either alone or with LPS (1 μg per mouse) (Sigma-Aldrich) by i.p. injection (primary immunization). On day 14, all mice received 100 μg OVA and 1 μg LPS via i.p. injection (boost). After an additional 5–7 d, mice were sacrificed, and sera were tested by ELISA for specific IgG anti-native OVA Abs.

Preparation of fluorochrome-labeled Ags

OVA and OVA$_{Cl}^{I}$ were transferred to 0.1 M sodium carbonate buffer by passage over a PD-10 Sephadex G-25 column. FITC (2 mg/ml) (Sigma-Aldrich) and tetramethylrhodamine isothiocyanate (TRITC) (6 mg/ml) (Fluka) in anhydrous DMSO (Acros Organics, Geel, Belgium) were prepared fresh. Fluorochromes were added slowly to the protein (50 μl per milligram of protein) and left for 4 h at room temperature in the dark. The unconjugated fluorochromes were removed by passage over a PD-10 Sephadex G-25 column to HBSS buffer. Dye-to-protein molar ratios were determined by absorbance measurements at 493 nm using a molar extinction coefficient of 72,000 M^{-1} cm^{-1} for FITC and at 555 nm using a molar extinction coefficient of 65,000 M^{-1} cm^{-1} for TRITC. FITC-OVA, TRITC-OVA, FITC-OVA$_{Cl}^{I}$, and TRITC-OVA$_{Cl}^{I}$ were stored at −20°C.

Ag uptake in vitro

Purified bone marrow-derived DCs were incubated with different doses of FITC-OVA or FITC-OVA$_{Cl}^{I}$ for the indicated time. Excess of Ag was removed by washing samples twice in ice-cold HBSS. Cells were fixed with 3.8% formaldehyde and analyzed on a FACScan (BD Biosciences, San Jose, CA) flow cytometer using CellQuest software or on a Leica confocal microscope (Leica Microsystems, Deerfield, IL) using the manufacturer's software.

Ag uptake in vivo

C57BL/6 mice were injected i.v. with 1 mg of FITC-OVA, or FITC-OVA$_{Cl}^{I}$ or an equal volume of HBSS. Spleens were collected at various time points, and CD11c^{+} DCs were purified as described above. DCs were stained for CD8a expression and then analyzed by flow cytometry.

Atomic force microscopy

Atomic force microscopy (AFM) tips were modified with a mixture of sulfonate-terminated thiol (sodium 2-mercapto-[^{1}H]benzo[*d*]imidazole-5-sulfonate) and OVA or OVA$_{Cl}^{I}$. Force–distance measurements were performed using Veeco PicoForce AFM (Santa Barbara, CA) by cycling the sample on a piezo scanner over 500–1000 nm in the vertical direction, varying the speed of the movement (loading rate) and the time that tips stay in contact with the surface (contact time). The final measurements were performed for the optimized loading rate (1000 nm/s) and contact time (1 s). If not specified, then all of the measurements were performed in PBS. The curves were measured on different areas of the macrophages immobilized on glass and on the glass surface itself as negative controls. One hundred to 300 curves were collected on each spot; the data were processed and averaged for the number of spots. The measurements for each condition were performed at least twice, changing the tip and the set of cells. For the given set of the curves, the adhesion probability was determined, where

$$\text{adhesion probability} = \text{number of curves with adhesion} / \text{number of all curves.}$$

Ag digestion

Digestion was performed at 37°C for 18 h. For trypsin digestion, OVA or OVA$_{Cl}^{I}$ (20 μg) was incubated with sequencing grade modified trypsin (1 μg) (Promega, Madison, WI) in 50 mM Tris-HCl and 10 mM $CaCl_2$ (pH 7.8). For cathepsin E digestion, OVA or OVA$_{Cl}^{I}$ (10 μg) was incubated with cathepsin E (R&D Systems, Minneapolis, MN) (10 ng) in 0.1 M NaOAc and 0.1 M NaCl (pH 3.5). For endoglycosidase F (PNGase F) digestion, OVA or OVA$_{Cl}^{I}$ (10 μg) was incubated with PNGase F (BioLabs) (1000 U) in G7 reaction buffer (New England BioLabs, Hitchin, U.K.).

Separation of proteins by SDS-PAGE

Proteins were separated using 4–12% NuPAGE Novex Bis-Tris minigels (Invitrogen). Samples were reduced by heating at 95°C for 5 min. Bands were visualized using silver (19) or Coomassie brilliant blue staining.

heat-killed B16 cells, or medium and then injected i.v. into C57BL mice (10^6 cells per mouse). Spleen cells were collected after 7 d, restimulated with medium or chlorinated B16 cells, and then assayed for IFN-γ responses to chlorinated B16 cells, Trp2 peptide (1 μg/ml), or medium by ELISpot as shown. The figure shows mean and SD of ELISpot values from triplicate wells from one representative experiment of three experiments.

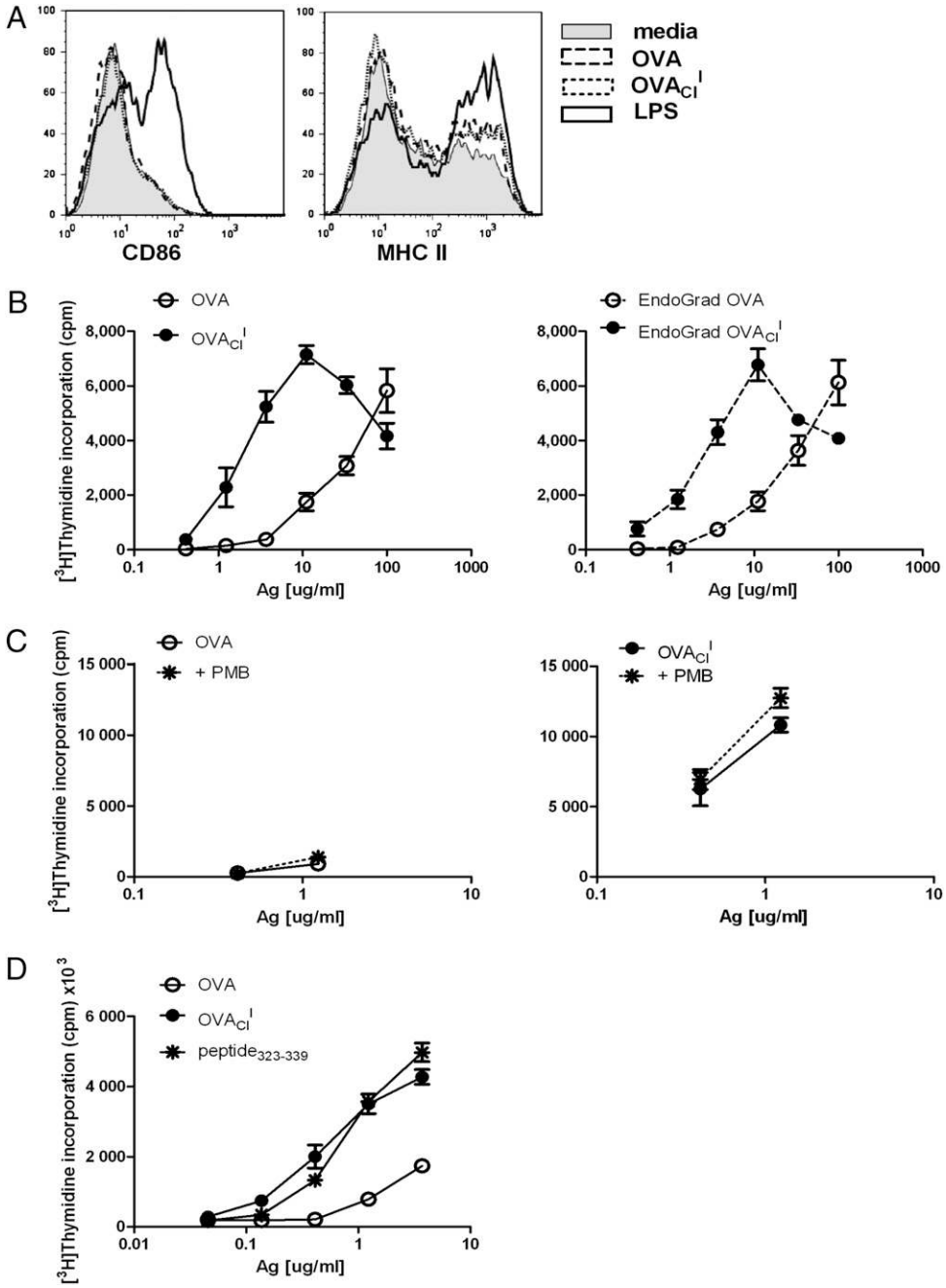

FIGURE 3. HOCl adjuvant activity is independent of TLR signaling. *A*, Bone marrow DCs were incubated for 18 h with OVA or OVA$_{Cl}^{I}$ (20 μg/ml, endotoxin-free) or LPS (100 ng/ml) and then analyzed for CD86 and MHC class II expression by flow cytometry. One representative experiment from three independent experiments is shown. *B*, TCR transgenic OT-II T cells were incubated with different concentrations of standard (grade V; Sigma-Aldrich) or endotoxin-free OVA or OVA$_{Cl}^{I}$ and bone marrow-derived DCs as described in *Materials and Methods*. The graph shows OTII proliferation measured as thymidine incorporation. One representative experiment from three independent experiments is shown. *C*, As for *B*, but cultures were performed in the presence or absence of polymyxin B (1 μg/ml). *D*, As for *B*, but Ag presentation assays were carried out using DCs from TRIF/MyD88 double-knockout mice. Results are presented as the average ± SD [^{3}H]thymidine incorporation of triplicate cultures. The experiment was repeated twice.

Results

HOCl modification facilitates processing and presentation to both CD4 and CD8 T cells

HOCl can cause a variety of covalent modifications to proteins (20, 21). One important reaction, which is straightforward to monitor, is the conversion of free α and ε amino side chains to the respective chloramines (Supplemental Fig. 1, Equation 1). These chloramines can be converted subsequently into free aldehydes (Supplemental Fig. 1, Equation 2) and ultimately oxidized irreversibly to carboxylic acids.

The model protein Ag OVA was reacted with various ratios of HOCl, and the extent of OVA modification was monitored by measuring the disappearance of free amines (Supplemental Fig. 1*A*) and the appearance of aldehydes (Supplemental Fig. 1*B*). Increasing amounts of HOCl induced a dose-dependent decrease in free amino groups. Concentrations of HOCl inducing a low (OVA$_{Cl}^{L}$), intermediate (OVA$_{Cl}^{I}$), or high (OVA$_{Cl}^{H}$) degree of free amino modification were tested in subsequent functional experiments. Increasing concentrations of HOCl also induced the appearance of free carbonyl groups, although these were produced at

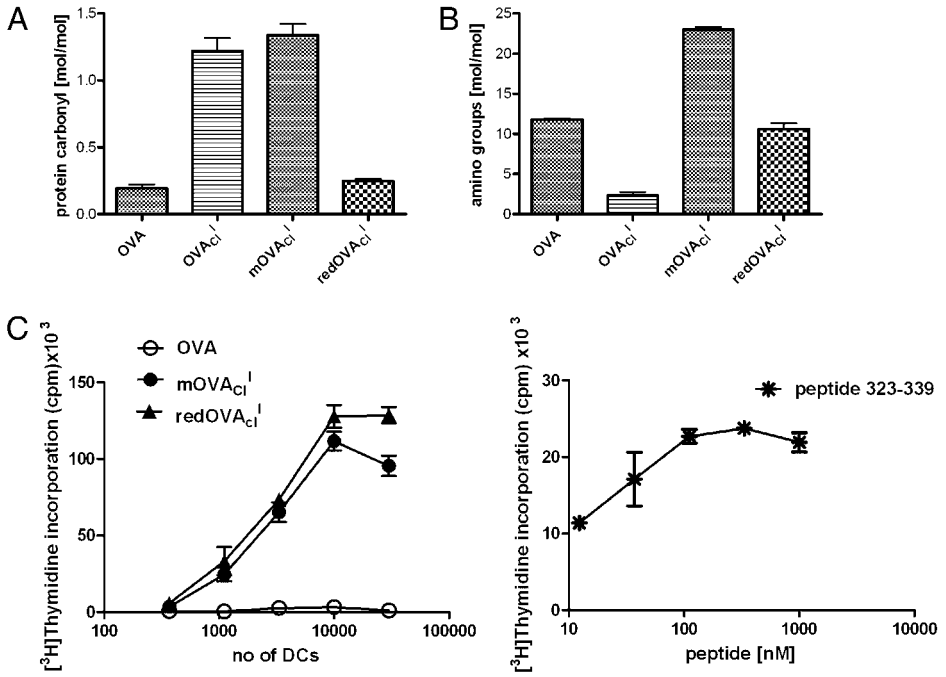

FIGURE 4. HOCl adjuvant activity does not require aldehyde or chloramine groups. *A*, Reaction with $NaBH_4$, but not methionine reduces the number of carbonyl groups on OVA_{Cl}^{I}. Mean ± SEM from three or more experiments. The carbonyl levels of OVA_{Cl}^{I} are significantly different from those of both OVA and OVA_{Cl}^{I} treated with $NaBH_4$ ($p < 0.01$, Student *t* test). *B*, Reaction with methionine, but not $NaBH_4$ restores free amine groups on OVA_{Cl}^{I}. Mean ± SEM from three or more experiments. The amine levels of OVA_{Cl}^{I} are significantly different from those of both OVA, and OVA_{Cl}^{I} treated with methionine ($p < 0.01$, Student *t* test). *C*, OVA_{Cl}^{I} was reacted with $NaBH_4$ or methionine as in *A* and *B* and then tested for processing and presentation in the OTII model as described in Fig. 1*C*. Results are presented as the average ± SD [^{3}H]thymidine incorporation (cpm) of the triplicate cultures. Experiment was repeated three times (*C*).

low frequency (maximum of 3 mol carbonyl/mol protein protein) and were only seen in OVA_{Cl}^{I} or OVA_{Cl}^{H}.

The effects of chlorination were tested initially in the well-characterized DO11.10 T cell hybridoma model (Fig. 1*A*). This hybridoma responds to intact OVA only after processing and presentation. DO11.10 responds poorly to native OVA, except at very high concentrations (>20 μM). In contrast, OVA_{Cl}^{I} induced a DO11.10 response even at concentrations of 0.2 μM. Both OVA_{Cl}^{L} and OVA_{Cl}^{H} were presented poorly. Efficient presentation of processed OVA_{Cl}^{I} could be detected after a lag phase of 2–3 h (Fig. 1*B*).

To exclude the possibility that this result was peculiar to the DO11.10 hybridoma, the experiment was repeated with T cells from the TCR transgenic mouse, OTII, which recognize the same sequence of OVA as DO11.10 (323–339), presented by I-A^b instead of I-A^d, and with a 200-fold greater sensitivity (Fig. 1*C*). In this case, native OVA processing could be detected at concentrations of 2 μM or above. However, as for DO11.10, processing of OVA_{Cl}^{I} was at least 10-fold more efficient (Fig. 1*C*), whereas OVA_{Cl}^{H} was processed and presented poorly (not shown). To exclude the possibility that the enhancement was due to a direct effect of traces of HOCl remaining in the chlorinated OVA preparations, DCs were treated directly with 5 μM HOCl. At these concentrations, HOCl was not toxic to the cells, but failed to induce any enhancement in Ag processing of OVA (Supplemental Fig. 2). Higher concentrations induced cellular cytotoxicity.

Although both DO11.10 and OTII showed a large increase in response to chlorinated OVA, this effect was not universal for all of the OVA epitopes (Fig. 1*D*). Indeed, the responses of two other T cell hybridomas, MF2.D9 (specific for OVA 273–288) and 3DO18.3 (specific for OVA 257–278), were abrogated almost completely by chlorination even at intermediate levels. Therefore, chlorination of OVA modifies the T cell response in an epitope-specific manner.

There is considerable evidence that particulate Ags are taken up and processed via different pathways from soluble Ags. Therefore, to compliment these studies on soluble Ags, the influence of chlorination was explored using a particulate Ag model. OVA or OVA_{Cl}^{I} was coated onto 1 μm beads. To facilitate the removal of excess beads before the addition of T cells, these experiments were carried out with macrophages rather than DCs. These experiments confirmed that the enhancement was not DC specific, because chlorination enhanced the processing and presentation of both soluble and bead-associated OVA by macrophages (Fig. 1*E*, 1*F*).

All of the T cells tested above are $CD4^+$ and recognize Ags after processing and loading onto class II MHC molecules. We wished to explore whether chlorination also facilitated cross-presentation via class I MHC molecules. However, preliminary experiments showed that the RF33 CD8 OVA-specific hybridoma behaved like the 3DO18.3 CD4 hybridoma (Fig. 1*D*) and did not recognize chlorinated OVA. The SIINFEKL epitope recognized by RF33 is within that recognized by the 3DO18.3 CD4 hybridoma and appears to be destroyed by chlorination.

Therefore, we used a different model for these cross-presentation experiments and studied the response to melanoma Ag Trp2, for which a CD8 class I epitope has been defined previously. DCs were incubated with B16.F10 melanoma cells expressing the Trp2 Ag (Supplemental Fig. 3), and injected i.v. into $H2^b$ mice. Two weeks later, splenic T cells were harvested and cultured in vitro, and the CD8 T cell response was measured by IFN-γ ELISpot (Fig. 1*G*). T cells from mice immunized with HOCl-modified B16.F10 cells, but not with B16.F10 cells killed by heat treatment or treatment with HCl (not shown) showed strong responses to the cross-presented Trp2 peptide coding for the major CD8 $H2^b$ epitope. Therefore, chlorination facilitates both direct processing of exogenous Ags to CD4 cells and cross-presentation of cell-associated Ag Trp2 to CD8 T cells.

Chlorinated OVA enhances the Ab response in vivo

Because chlorination enhanced presentation of some OVA epitopes to CD4 cells in vitro, we next explored the effect of this process on OVA Ab responses, which are CD4 T cell dependent. Because many previous studies have demonstrated that for an efficient Ab response an innate immune stimulant or adjuvant is required (22), mice were primed with OVA/OVA_{Cl}^{I}, with and without LPS. As expected, OVA without LPS stimulated a small IgG response (Fig. 2*A*). In contrast, OVA_{Cl}^{I} stimulated a significant Ab response, even in the absence of LPS. Immunization with OVA and LPS stimulated a much stronger response than OVA alone, and this was enhanced further by moderate chlorination (Fig. 2*B*).

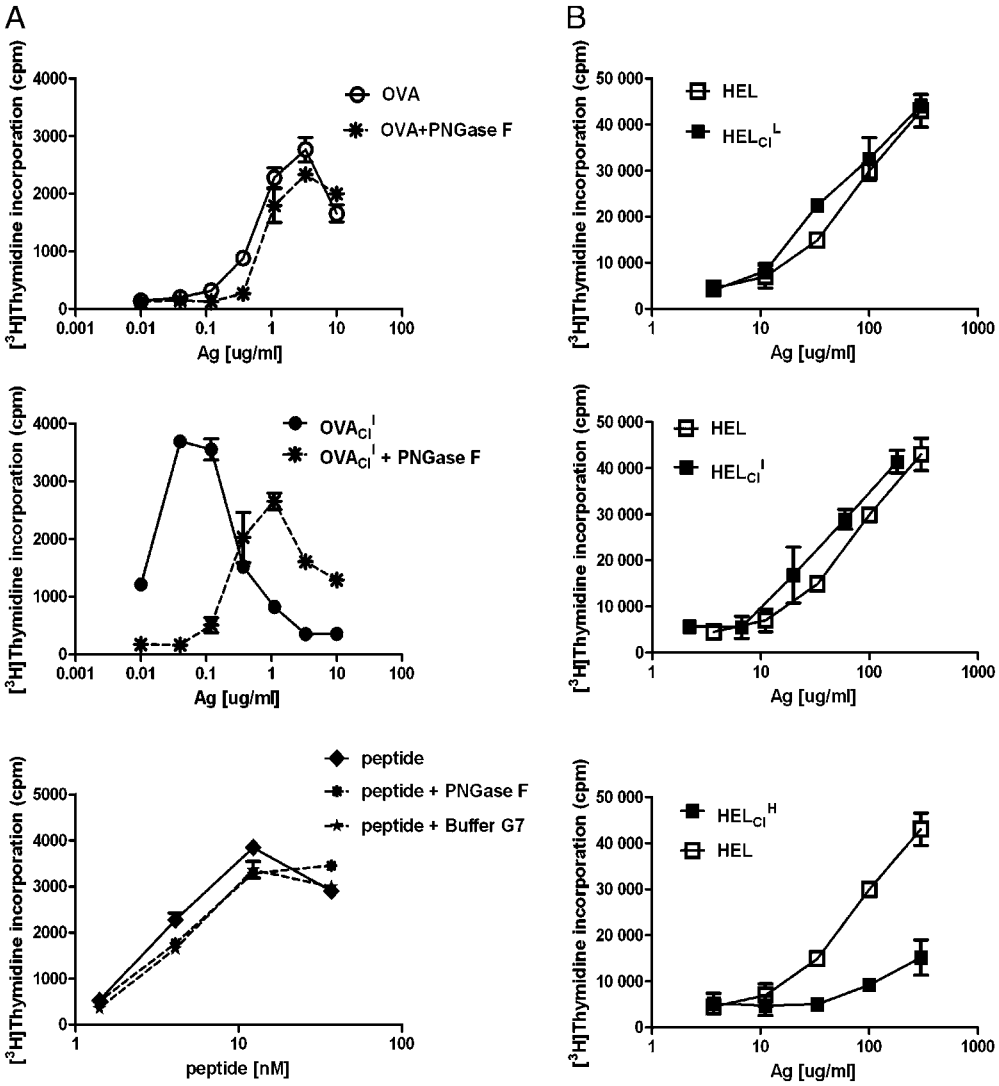

FIGURE 5. HOCl adjuvant activity requires the OVA carbohydrate side chain. *A*, OVA, OVA$_{Cl}^{I}$, or OVA 323–339 peptide was treated with PNGase F and then tested for processing and presentation in the OTII model as described in Fig. 2*C*. Results are presented as the average ± SD [^{3}H]thymidine incorporation of triplicate cultures. The experiment was repeated twice. *B*, HEL was oxidized at low, intermediate, and high concentrations of HOCl and tested using the lysozyme-specific hybridoma Ad71–85 as described in *Materials and Methods*. The graph shows IL-2 release measured as thymidine incorporation of the CTLL-2 indicator cell line. The experiment was repeated three times.

Immunization with OVA$_{Cl}^{H}$ induced very little Ab response even in the presence of LPS. Interestingly, chlorination induced only a moderate (~2-fold) increase of anti-OVA IgG1, which is the major default isotype in BALB/c mice (Fig. 2*C*), whereas the Ig2a OVA-specific response is enhanced >10-fold (Fig. 2*D*). The increased Ig2a/IgG1 ratio is characteristic of a Th2/Th1 shift.

Enhancement of OVA via chlorination is not mediated via TLRs

There is considerable literature that emphasizes the need for cooperative stimulation of immunity between TLR ligands such as LPS and cognate Ags such as OVA. Trace amounts of TLR ligands, which are often found as contaminants of Ag preparations, may be sufficient to influence the outcome. Therefore, it is possible that chlorination might act via enhancing either the TLR response or the sensitivity of the OVA response to TLR ligation. Alternatively, chlorination might bypass the need for the TLR component. These alternative hypotheses were addressed in a number of ways.

Coculture of either OVA or OVA$_{Cl}^{I}$ with DCs was used as a sensitive bioassay of LPS activity. Neither OVA nor OVA$_{Cl}^{I}$ induced DC maturation (Fig. 3*A*), confirming the absence of any biologically active TLR ligand in the preparations.

Next, the functional experiments were repeated with endotoxin-free OVA. However, the enhancement of the T cell response due to chlorination was equivalent irrespective of whether this endotoxin-free OVA or the conventional preparation was used (Fig. 3*B*). Furthermore, the enhancement was not affected by the addition of polymyxin B, an inhibitor of LPS (Fig. 3*C*). Finally, we tested OVA and OVA$_{Cl}^{I}$ using DCs isolated from TRIF/MyD88 double-knockout mice (Fig. 3*D*), in which both major signaling TLR pathways are blocked. The absence of these two key TLR downstream signaling adaptors did not affect the enhanced processing and presentation of the chlorinated OVA.

Enhancement of OVA via chlorination is not mediated via aldehyde or chloramine functional groups, but requires the carbohydrate side chain

Because HOCl-dependent enhancement of Ag processing was not mediated via TLRs, we examined other possible mechanisms that might underlie the phenomenon. One such mechanism is protein modification by introduction of aldehyde groups, which can enhance both uptake and processing (23, 24). As shown in Supplemental Fig. 1, HOCl treatment does result in the introduction of aldehyde groups

via amine oxidation. However, reduction of aldehydes in OVA_{Cl}^{I} by treatment with $NaBH_4$ (Fig. 4*A*) did not reverse the enhancement in T cell response (Fig. 4*C*). Thus, aldehyde groups were not required for HOCl-induced enhancement of processing.

Chloramines, another major product of protein chlorination, were also not required, because reduction of chloramines back to amines by methionine did not reverse the enhanced T cell response (Fig. 4*C*). The number of free accessible amines in OVA_{Cl}^{I} after methionine reduction was greater than that for native OVA, suggesting that oxidation altered protein confirmation and allowed access to previously inaccessible amine side chains.

The OVA protein contains a single N-linked carbohydrate side chain at asparagine 293. The side chain is made up principally of mannose and *N*-acetyl glucosamine residues (25). More recent studies also suggest the presence of some terminal sialic acid residues (26). *N*-Acetyl glucosamine is a major target for HOCl modification, leading to the production of a whole variety of oxidized sugar products (27). Therefore, we explored the possibility that a component of the carbohydrate side chain was important for the adjuvant effects of HOCl. Both OVA and OVA_{Cl}^{I} were treated with PNGase F, which removes the entire carbohydrate side chain (Supplemental **F**ig. 4). Enzyme treatment had no effect on the presentation of native OVA or OVA peptide, but abolished the enhancement that resulted from chlorination (Fig. 5*A*, *middle panel*). In contrast, treatment with neuraminidase (which selectively removes sialic acid residues) had no effect on presentation of either OVA or OVA_{Cl}^{I} (not shown).

To confirm the importance of the carbohydrate side chain, we repeated the chlorination experiments using a nonglycosylated protein Ag, lysozyme (Fig. 5*B*). Chlorination at low and medium ratios had no effect on presentation of lysozyme to a lysozyme-specific hybridoma. Similarly to OVA, chlorination using a high ratio of HOCl decreased the response.

Chlorination enhances APC uptake of OVA

The chemical modification of OVA, and specifically of its carbohydrate side chain, might alter the handling of Ag by the APC. We therefore examined the uptake of OVA_{Cl}^{I} by DCs. Bone marrow DCs were incubated with different concentrations of FITC-labeled OVA and OVA_{Cl}^{I} for 2 h (Fig. 6*A*). Chlorination enhanced uptake over a wide range of Ag concentrations. Confocal analysis of the DCs confirmed that both labeled OVA and OVA_{Cl}^{I} were taken up into endocytic vesicles inside the cell (Fig. 6*B*). Images of simultaneous uptake of OVA-FITC and OVA_{Cl}^{I}-TRITC showed extensive colocalization of the two fluorophores, suggesting that chlorination

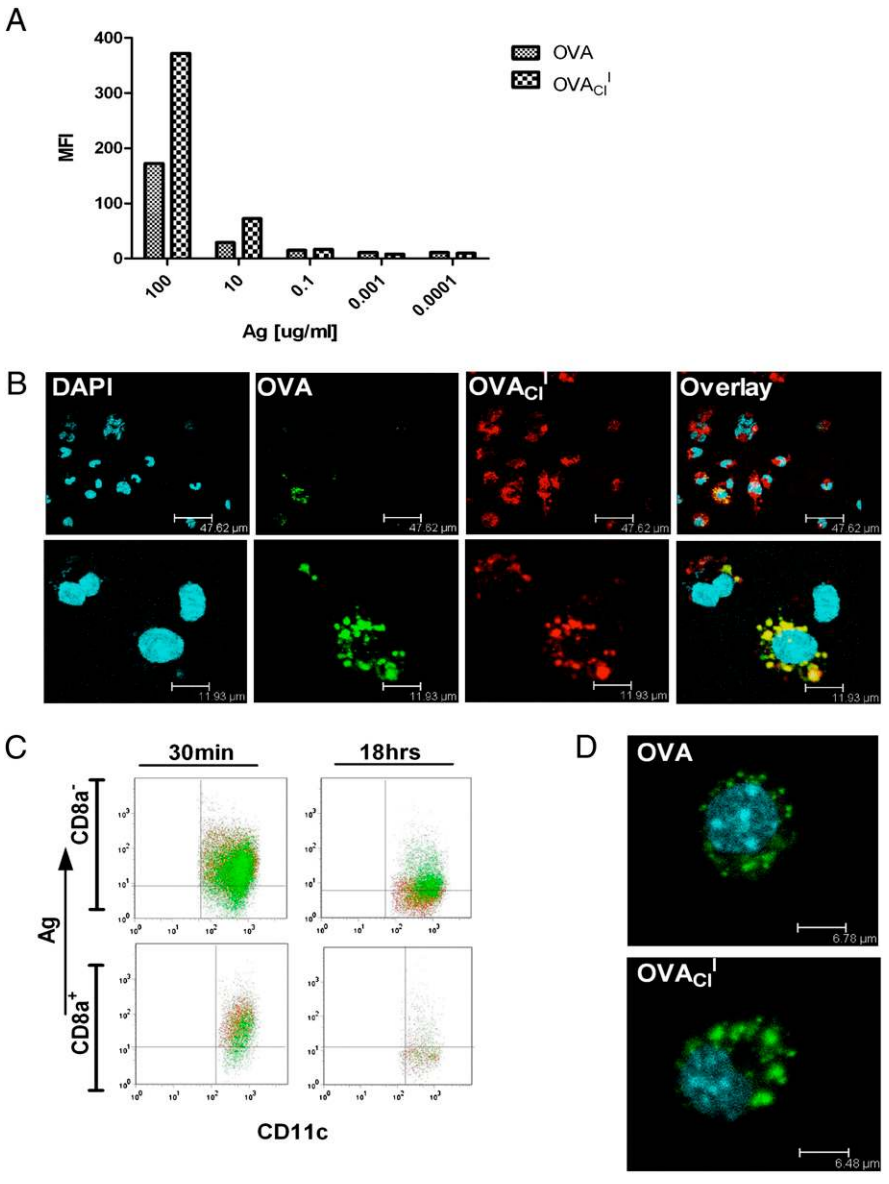

FIGURE 6. Modification with HOCl facilitates uptake and processing of OVA. *A*, Bone marrow-derived DCs were incubated with different concentrations of OVA or OVA_{Cl}^{I} conjugated with FITC for 2 h at 37°C. Free soluble Ag was removed, and the cells were fixed in 3.8% formaldehyde. Fluorescence was analyzed by flow cytometry. The graph shows median fluorescent intensity of the DC population in the FITC channel and is one representative experiment from three independent experiments. The two distributions are significantly different ($p < 0.01$, χ^2 test). *B*, Bone marrow-derived DCs were incubated with OVA-FITC and OVA_{Cl}^{I}-TRITC (100 μg/ml) for 2 h at 37°C. Excess Ag was removed, and the cells were fixed in 3.8% formaldehyde. Fluorescence was analyzed by confocal microscopy. The figure shows a representative low-power (*upper row*) image and a high-power image of a cell that has taken up both Ags. The experiment was repeated three times. *C*, C57BL mice were injected i.v. with OVA or OVA_{Cl}^{I} conjugated with FITC (1 mg per mouse). Spleen cells were collected after 30 min or 18 h, and CD11c DCs were isolated by magnetic bead enrichment. The splenic DCs were stained for CD11c and CD8a. The plots show an overlay of OVA-FITC (green) and OVA_{Cl}^{I}-FITC (red) for $CD8a^+$ and $CD8^-$ DCs. *D*, Confocal analysis of cells from the 30-min time point to demonstrate intracellular localization of OVA and OVA_{Cl}^{I}. Experiments were repeated three times; each time three mice per group were injected. One representative mouse from each group is shown (*C*, *D*).

enhances the magnitude of Ag uptake, but does not substantially alter intracellular routing.

The uptake of OVA and OVA_{Cl}^{I} also was investigated in vivo. Both OVA and OVA_{Cl}^{I} could be detected within splenic CD11c DCs following i.v. injection of Ag (Fig 6*C*, 6*D*). There was a moderate enhancement in the uptake of OVA_{Cl}^{I} at 30 min postinjection in both $CD8^{+}$ and $CD8^{-}$ $CD11c^{+}$ populations. Interestingly, at 18 h postinjection, the situation was reversed, and the OVA_{Cl}^{I} signal was close to that of the background, consistent with a more rapid processing and degradation of the chlorinated Ag.

Chlorination facilitates proteolysis of OVA

On the basis of the findings shown in Fig. 6, the relative susceptibilities of OVA and chlorinated OVA to proteolysis were investigated. The 323–339 sequence recognized by the DO11.10 and OT-II hybridomas is buried within the hydrophobic core of the OVA molecule (Supplemental Fig. 5), and extensive proteolysis or fragmentation is required to release this sequence for MHC loading (28). Although HOCl itself at very high concentrations can cause protein fragmentation, no low molecular weight protein fragments could be detected with PAGE of OVA_{Cl}^{I} (Fig. 7*A*), consistent with earlier studies showing a lack of protein fragmentation at these levels of HOCl (29). Furthermore, OVA_{Cl}^{I}, like native OVA, could not be presented by fixed DCs (Fig. 7*B*), and processing of OVA_{Cl}^{I} was sensitive to the cathepsin D/E inhibitor MPC6, which has been shown to block processing and presentation of native OVA (Supplemental **F**ig. 6).

Nevertheless, although chlorination at low and intermediate ratios does not induce any extensive fragmentation by itself, it does alter the susceptibility of OVA to proteolysis. Native OVA itself is highly resistant to proteolytic degradation by either trypsin or cathepsin E, an aspartic proteinase required for OVA processing by DCs (18). In contrast, OVA_{Cl}^{I} is digested by both cathepsin E (Fig. 7*C*) and trypsin (Fig. 7*D*).

Chlorination enhances APC binding of OVA via specific receptor(s)

The flow cytometry and confocal studies demonstrate increased uptake, but cannot address the interaction between OVA and the APC surface. Lowering the temperature to 4°C completely blocked uptake. At this temperature, however, DCs gave only a very slight fluorescent signal when they were incubated with either labeled OVA_{Cl}^{I} or OVA (Supplemental Fig. 7). This technique therefore was not suitable for measuring binding parameters.

Instead, we used AFM (30) to measure directly the binding of OVA and OVA_{Cl}^{I} with fixed APCs. Macrophages rather than DCs had to be used for these studies, because the weak interaction of DCs with the substrate prevented us from obtaining reproducible results. OVA, OVA_{Cl}^{I}, or OVA_{Cl}^{H} were coated onto gold AFM probes, and the strength of the binding interaction to the surface of macrophages was quantified by measuring the adhesion probability as the probe was lowered and raised from the macrophage surface.

OVA binding to the macrophage surface was close to background values, whereas both OVA_{Cl}^{I} and OVA_{Cl}^{H} showed enhanced binding (Fig. 8*A*). Analysis of force-distance graphs for individual binding events for OVA_{Cl}^{I} were consistent with a single OVA/receptor rupture event (Fig. 8*B*). In contrast, the graphs for OVA_{Cl}^{H} suggested that each binding event was made up of multiple rupture events (not shown), consistent with the model that high concentrations of HOCl induce protein fragmentation. The binding forces measured for OVA_{Cl}^{I} were on the order of several hundred piconewtons, consistent with a single or small number of Ag/receptor interactions per rupture event. Preincubation of macrophages in the presence of increasing concentrations of OVA_{Cl}^{I} decreased the adhesion probability down to ~30% (Fig. 8*C*), the same value as that found for binding of OVA_{Cl}^{I} or OVA_{Cl}^{H} to fibroblasts. The enhanced binding of OVA_{Cl}^{I} to macrophages is therefore predominantly receptor-mediated. In contrast, the binding of OVA_{Cl}^{H} is likely mediated by numerous nonspecific interactions of fragmented or denatured protein.

One possible receptor that might be implicated in the binding of OVA and OVA_{Cl}^{I} is the lectin-like oxidized low-density lipoprotein receptor (Lox-1), which is expressed on both DCs and macrophages (31) and which has been implicated previously in binding to chlorinated macromolecules (32). To test whether Lox-1 mediates enhanced uptake of OVA_{Cl}^{I}, we incubated FITC-labeled OVA and OVA_{Cl}^{I} with Lox-1–expressing or control Chinese hamster ovary cells (Fig. 8*D*). The expression of Lox-1 enhanced uptake of both OVA and OVA_{Cl}^{I}, but OVA_{Cl}^{I} was taken up more efficiently (Supplemental Fig. 8). However, although we confirmed the presence of

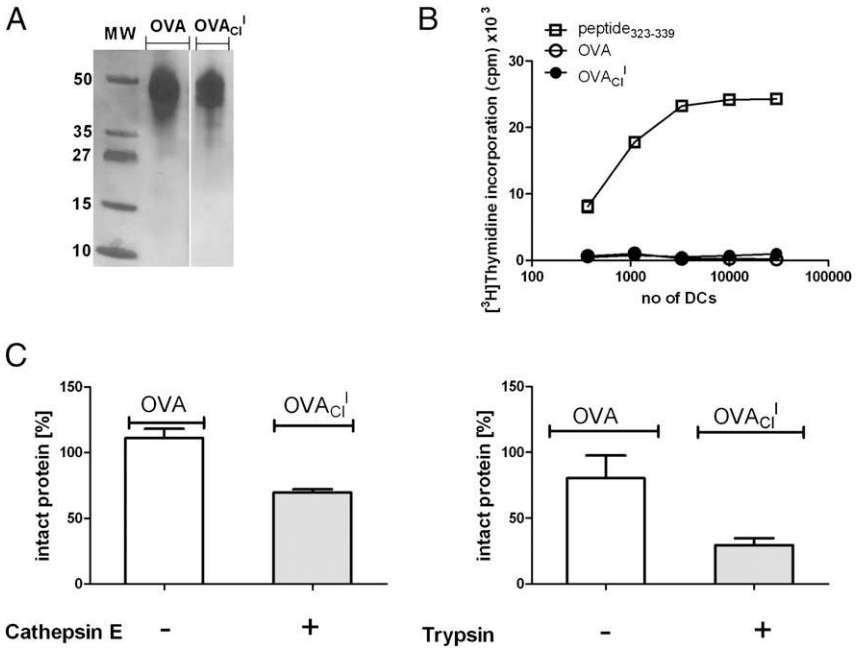

FIGURE 7. Modification with HOCl increases the proteolytic susceptibility of OVA. *A*, OVA and OVA_{Cl}^{I} (5 μg) were fractionated by 4–12% gradient PAGE, and the gel was stained with silver stain. No low molecular weight fragments were visible. The experiment was repeated three times. *B*, OVA (250 μg/ml), OVA_{Cl}^{I} (250 μg/ml), or OVA 323–339 peptide (1 μg/ml) were incubated with glutaraldehyde-fixed DCs and DO11.10 T hybridoma cells, and IL-2 release was measured as described in Fig. 1*A*. Results are presented as the average ± SD [^{3}H]thymidine incorporation of triplicate cultures. The experiment was repeated twice. *C* and *D*, OVA and OVA_{Cl}^{I} were digested with cathepsin E (*C*) or trypsin (*D*) as described in *Materials and Methods* and analyzed by 4–12% gradient denaturing PAGE. Histograms show the degree of proteolysis quantified by comparing the intensity of the OVA bands before and after digestion using densitometry. Results are presented as the average ± SEM of three independent experiments. The difference between OVA and OVA_{Cl}^{I} are significant at $p < 0.05$ (Student *t* test, $n = 3$).

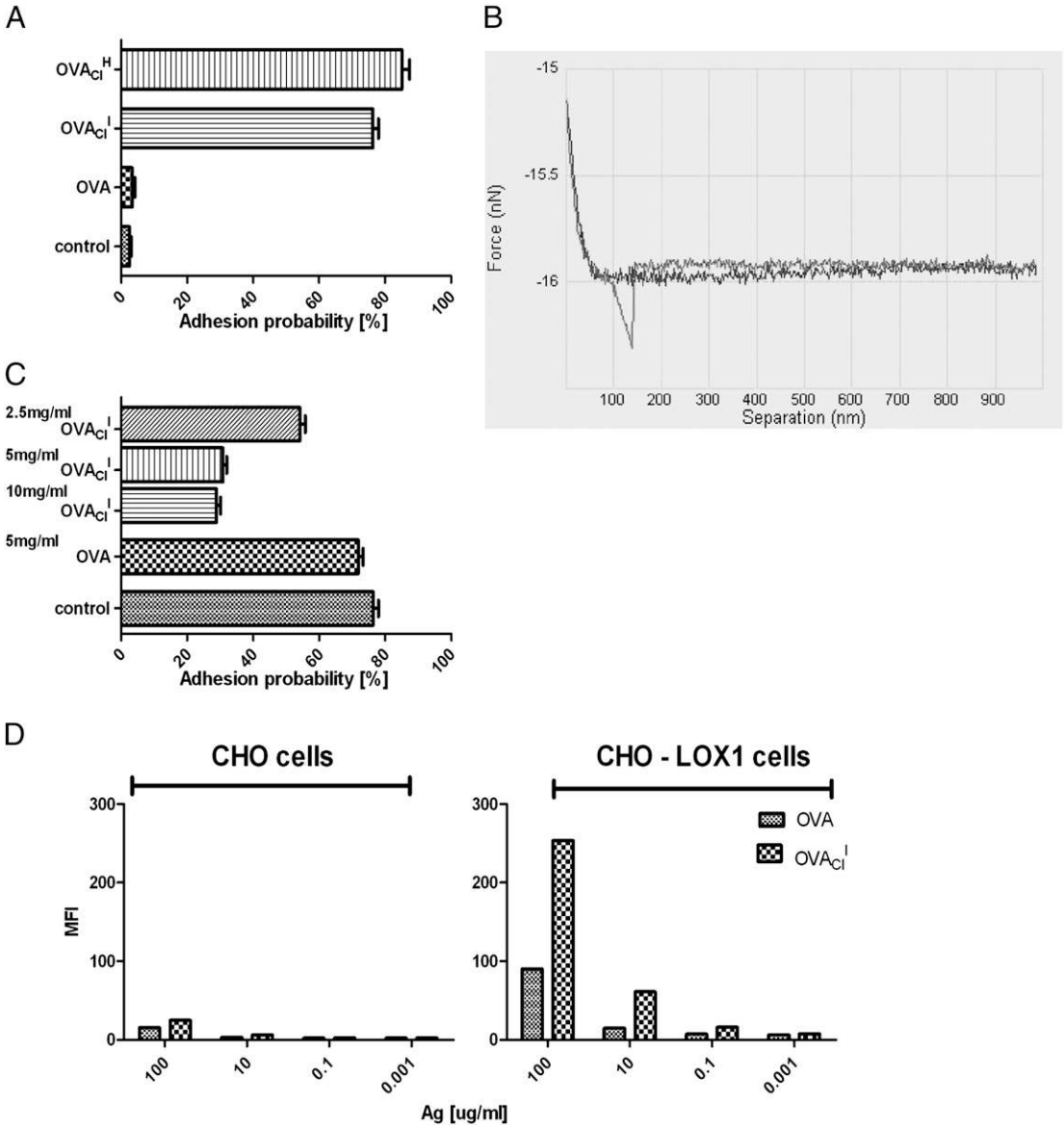

FIGURE 8. Chlorinated OVA binds preferentially to receptors on the cell surface. *A*, The interaction of OVA, OVA_{Cl}^{I}, and OVA_{Cl}^{H} bound to the surface of a probe, with the surface of macrophages was measured by AFM as described in *Materials and Methods*. *B*, A representative force-distance curve from one individual AFM measurement showing the characteristic profile of a single OVA/receptor rupture. *C*, The binding of OVA_{Cl}^{I} was measured by AFM as in *A*, but cells were preincubated in OVA (5 mg/ml) or different concentrations of OVA_{Cl}^{I}. *D*, OVA or OVA_{Cl}^{I} conjugated with FITC was incubated at different concentrations with Chinese hamster ovary cells expressing the Lox-1 scavenger receptor or control untransfected cells. After 30 min, the excess Ag was removed, and the cells were fixed in 3.8% formaldehyde and analyzed by flow cytometry. The results are expressed as median fluorescent intensity in the FITC channel and are one representative of three independent experiments. The difference between the oxidized and nonoxidized profiles is significant for the Lox-1–transfected cells ($p < 0.01$), but not the control cells ($p = 0.15$) (χ^2).

low levels of Lox-1 on bone marrow-derived DCs by flow cytometry, we were unable to block the presentation of either OVA or OVA_{Cl}^{I} using Abs against the Lox-1 receptor (not shown). Thus, Lox-1 may contribute to the enhanced uptake of OVA_{Cl}^{I}, but the uptake is likely to involve multiple redundant receptors on the DC surface.

Discussion

Protein chlorination is a recognized hallmark of the inflammatory response (10) and contributes to neutrophil microbicidal activity as well as to inflammatory immunopathology. Chlorination also can lead to inflammatory enzyme inactivation (33) and thus regulate inflammation negatively. The influence of protein chlorination on adaptive immunity, however, has received relatively little attention. The hypothesis underlying this study, based on earlier studies (34, 35), was that chlorination might act as a natural adjuvant, facilitating recognition by APCs and hence enhancing the overall immune response.

The data presented in this article show that protein chlorination fulfills several of the criteria required for an adjuvant. Both DCs and macrophages processed and presented chlorinated OVA to DO11.10 and OTII T cells with increased efficiency. Indeed, in the case of the DO11.10 hybridoma, chlorination was essential to allow processing within physiological concentrations of Ag. The concentrations of HOCl present in vivo are difficult to determine, because they are confounded by the presence of scavengers, by rapid diffusion, and by spontaneous conversion into other species (36). However, the presence of protein modifications that result from myeloperoxidase-dependent HOCl oxidation have been extensively documented in vivo, both within the neutrophil phagolysosome (37, 38) and in the

extracellular inflammatory milieu (38, 39). Thus, Ag modification by this route is a likely event during neutrophil activation.

Processing and presentation occurred independent of TLR signaling, which previously has been shown to be required to trigger Ag processing (8). Chlorination also enhanced Ag processing via the cross-priming class I pathway, although further studies will be required to determine how general this phenomenon is. Furthermore, the increased processing and presentation due to chlorination resulted in enhanced immune effector function, in terms of both Ab response and class I restricted IFN-γ–producing effector cells. Interestingly, the shift in isotype of the Ab response was consistent with a Th2/Th1 shift, which may reflect an increased epitope density on the surfaces of APCs resulting from enhanced uptake and processing (40).

The adjuvant effect of HOCl is tempered by its potential to damage proteins. It is therefore possible that epitopes that are recognized by the adaptive immune response could be destroyed by chlorination. In fact, the epitopes recognized by two CD4 (3DO18.3 and MF2.2D9) and one CD8 (RF33) TCRs tested are particularly sensitive to HOCl modification. This could be either because they contain methionines whose side chains are known to be the primary targets of HOCl (41–43) or because of their exposed position on the surface of the OVA molecule (Supplemental Fig. 5).

Higher HOCl-to-protein ratios reduced the response of all of the T cells tested as well as the Ab response. High concentrations of HOCl not only modify an increasing range of amino acid side chains, but also result in formation of active radical centers on nitrogens and carbons of the protein backbone (44). These radical centers induce further rearrangements that can result in extensive protein fragmentation and denaturation and associated loss of immunogenicity. The ability to enhance immune responses and in parallel to destroy epitope recognition is reminiscent of the effects of formaldehyde, whose adjuvant properties have long been incorporated into vaccine formulations (24). However, in contrast to formaldehyde, the adjuvant effect of HOCl is not mediated via protein aldehyde groups, and indeed aldehyde formation is limited at the ratios of HOCl giving optimum immune responses. Instead, HOCl adjuvant effects are dependent upon the presence of the asparagine-linked carbohydrate side chain. *N*-Acetyl glucosamine is a major component of this structure and is also a major target for HOCl (25), which converts this sugar into a whole range of oxidized products (45). Therefore, the carbohydrate side chain in OVA_{Cl}^{I} may contain a very high density of oxidation products and hence provide an efficient and accessible ligand for appropriate receptors.

At least two mechanisms have been identified that may contribute to the adjuvant effects of HOCl. Chlorinated OVA as well as chlorinated cells (46) are taken up more efficiently than native OVA. Enhanced uptake is mediated by stronger binding to the cell membrane, which is of too low affinity to be detected by flow cytometry, but could be detected by direct measurement using AFM. Furthermore, the binding is mediated via specific receptors, because it is inhibited by excess ligand. The scavenger receptor Lox-1 can contribute to binding, but several other members of the scavenger receptor family as well as receptor for advanced glycation endoproducts receptor families have been implicated in recognition of oxidized macromolecules, and the overall binding interaction is likely to show considerable redundancy.

In addition to enhanced uptake, HOCl also enhances the sensitivity of OVA to proteolysis. The known reactivity of HOCl with cystine disulfide bonds as well as the increased accessibility of ε amino groups in OVA_{Cl}^{I} suggest that this increased susceptibility results from a more relaxed open three-dimensional structure. It is tempting to speculate that this enhanced susceptibility to proteolysis also contributes to more efficient processing and presentation. However, one recent study has reported that enhanced proteolysis decreases immunogenicity by decreasing the $t_{1/2}$ of Ag within the APC (47). Our data suggest that the overall efficiency of the processing pathway is determined by a balance between the efficiency with which epitopes are released from intact proteins and the rate at which the epitopes are destroyed by further degradation. Therefore, we suggest that the net effects of chlorination may vary between different Ags.

Conclusion

This study demonstrates that protein chlorination can act as a natural adjuvant of immune responses to proteins, leading to enhanced processing, presentation, and effector responses. It is becoming clear that man-made adjuvants, many of which have been used for over a century with little understanding of their mode of action, act predominantly by stimulating cross-talk between innate and adaptive immunity. In a similar way, HOCl, a product of innate immune activation, can be considered a natural adjuvant, facilitating the subsequent recognition and processing of Ags by APCs, and hence stimulating a more effective adaptive immune response. Further studies are in progress to harness the adjuvant activity of HOCl to improve the immune response to tumor-associated Ags and hence develop effective strategies for cancer immunotherapy (46, 48).

Disclosures

The authors have no financial conflicts of interest.

References

1. Fearon, D. T., and R. M. Locksley. 1996. The instructive role of innate immunity in the acquired immune response. *Science* 272: 50–53.
2. Pasare, C., and R. Medzhitov. 2005. Control of B-cell responses by Toll-like receptors. *Nature* 438: 364–368.
3. Eisenbarth, S. C., O. R. Colegio, W. O'Connor, F. S. Sutterwala, and R. A. Flavell. 2008. Crucial role for the Nalp3 inflammasome in the immunostimulatory properties of aluminium adjuvants. *Nature* 453: 1122–1126.
4. Sallusto, F., and A. Lanzavecchia. 1994. Efficient presentation of soluble antigen by cultured human dendritic cells is maintained by granulocyte/macrophage colony-stimulating factor plus interleukin 4 and downregulated by tumor necrosis factor α. *J. Exp. Med.* 179: 1109–1118.
5. Trombetta, E. S., M. Ebersold, W. Garrett, M. Pypaert, and I. Mellman. 2003. Activation of lysosomal function during dendritic cell maturation. *Science* 299: 1400–1403.
6. Cumberbatch, M., R. J. Dearman, and I. Kimber. 1997. Interleukin 1β and the stimulation of Langerhans cell migration: comparisons with tumour necrosis factor α. *Arch. Dermatol. Res.* 289: 277–284.
7. Trombetta, E. S., and I. Mellman. 2005. Cell biology of antigen processing in vitro and in vivo. *Annu. Rev. Immunol.* 23: 975–1028.
8. Blander, J. M., and R. Medzhitov. 2006. Toll-dependent selection of microbial antigens for presentation by dendritic cells. *Nature* 440: 808–812.
9. Drakesmith, H., D. O'Neil, S. C. Schneider, M. Binks, P. Medd, E. Sercarz, P. Beverley, and B. Chain. 1998. In vivo priming of T cells against cryptic determinants by dendritic cells exposed to interleukin 6 and native antigen. *Proc. Natl. Acad. Sci. USA* 95: 14903–14908.
10. Klebanoff, S. J. 2005. Myeloperoxidase: friend and foe. *J. Leukoc. Biol.* 77: 598–625.
11. Malle, E., G. Marsche, J. Arnhold, and M. J. Davies. 2006. Modification of low-density lipoprotein by myeloperoxidase-derived oxidants and reagent hypochlorous acid. *Biochim. Biophys. Acta* 1761: 392–415.
12. Hawkins, C. L., and M. J. Davies. 2005. Inactivation of protease inhibitors and lysozyme by hypochlorous acid: role of side-chain oxidation and protein unfolding in loss of biological function. *Chem. Res. Toxicol.* 18: 1600–1610.
13. Woods, A. A., and M. J. Davies. 2003. Fragmentation of extracellular matrix by hypochlorous acid. *Biochem. J.* 376: 219–227.
14. Alderman, C. J., P. R. Bunyard, B. M. Chain, J. C. Foreman, D. S. Leake, and D. R. Katz. 2002. Effects of oxidised low density lipoprotein on dendritic cells: a possible immunoregulatory component of the atherogenic micro-environment? *Cardiovasc. Res.* 55: 806–819.
15. Dalle-Donne, I., R. Rossi, D. Giustarini, A. Milzani, and R. Colombo. 2003. Protein carbonyl groups as biomarkers of oxidative stress. *Clin. Chim. Acta* 329: 23–38.
16. Barnden, M. J., J. Allison, W. R. Heath, and F. R. Carbone. 1998. Defective TCR expression in transgenic mice constructed using cDNA-based α- and β-chain genes under the control of heterologous regulatory elements. *Immunol. Cell Biol.* 76: 34–40.
17. Free, P., C. A. Hurley, T. Kageyama, B. M. Chain, and A. B. Tabor. 2006. Mannose-pepstatin conjugates as targeted inhibitors of antigen processing. *Org. Biomol. Chem.* 4: 1817–1830.

18. Chain, B. M., P. Free, P. Medd, C. Swetman, A. B. Tabor, and N. Terrazzini. 2005. The expression and function of cathepsin E in dendritic cells. *J. Immunol.* 174: 1791–1800.
19. Nesterenko, M. V., M. Tilley, and S. J. Upton. 1994. A simple modification of Blum's silver stain method allows for 30 minute detection of proteins in polyacrylamide gels. *J. Biochem. Biophys. Methods* 28: 239–242.
20. Pattison, D. I., C. L. Hawkins, and M. J. Davies. 2007. Hypochlorous acid-mediated protein oxidation: how important are chloramine transfer reactions and protein tertiary structure? *Biochemistry* 46: 9853–9864.
21. Stadtman, E. R., and R. L. Levine. 2003. Free radical-mediated oxidation of free amino acids and amino acid residues in proteins. *Amino Acids* 25: 207–218.
22. Bonifaz, L., D. Bonnyay, K. Mahnke, M. Rivera, M. C. Nussenzweig, and R. M. Steinman. 2002. Efficient targeting of protein antigen to the dendritic cell receptor DEC-205 in the steady state leads to antigen presentation on major histocompatibility complex class I products and peripheral $CD8^+$ T cell tolerance. *J. Exp. Med.* 196: 1627–1638.
23. Allison, M. E., and D. T. Fearon. 2000. Enhanced immunogenicity of aldehyde-bearing antigens: a possible link between innate and adaptive immunity. *Eur. J. Immunol.* 30: 2881–2887.
24. Moghaddam, A., W. Olszewska, B. Wang, J. S. Tregoning, R. Helson, Q. J. Sattentau, and P. J. Openshaw. 2006. A potential molecular mechanism for hypersensitivity caused by formalin-inactivated vaccines. *Nat. Med.* 12: 905–907.
25. Harvey, D. J., D. R. Wing, B. Küster, and I. B. Wilson. 2000. Composition of N-linked carbohydrates from ovalbumin and co-purified glycoproteins. *J. Am. Soc. Mass Spectrom.* 11: 564–571.
26. Lattova, E., H. Perreault, and O. Krokhin. 2004. Matrix-assisted laser desorption/ionization tandem mass spectrometry and post-source decay fragmentation study of phenylhydrazones of N-linked oligosaccharides from ovalbumin. *J. Am. Soc. Mass Spectrom.* 15: 725–735.
27. Jahn, M., J. W. Baynes, and G. Spiteller. 1999. The reaction of hyaluronic acid and its monomers, glucuronic acid and *N*-acetylglucosamine, with reactive oxygen species. *Carbohydr. Res.* 321: 228–234.
28. Chesnut, R. W., and H. M. Grey. 1981. Studies on the capacity of B cells to serve as antigen-presenting cells. *J. Immunol.* 126: 1075–1079.
29. Olszowski, S., E. Olszowska, T. Stelmaszyńska, A. Krawczyk, J. Marcinkiewicz, and N. Baczek. 1996. Oxidative modification of ovalbumin. *Acta Biochim. Pol.* 43: 661–672.
30. Hinterdorfer, P., and Y. F. Dufrêne. 2006. Detection and localization of single molecular recognition events using atomic force microscopy. *Nat. Methods* 3: 347–355.
31. Delneste, Y., G. Magistrelli, J. Gauchat, J. Haeuw, J. Aubry, K. Nakamura, N. Kawakami-Honda, L. Goetsch, T. Sawamura, J. Bonnefoy, and P. Jeannin. 2002. Involvement of LOX-1 in dendritic cell-mediated antigen cross-presentation. *Immunity* 17: 353–362.
32. Dunn, S., R. S. Vohra, J. E. Murphy, S. Homer-Vanniasinkam, J. H. Walker, and S. Ponnambalam. 2008. The lectin-like oxidized low-density-lipoprotein receptor: a pro-inflammatory factor in vascular disease. *Biochem. J.* 409: 349–355.
33. Wang, Y., H. Rosen, D. K. Madtes, B. Shao, T. R. Martin, J. W. Heinecke, and X. Fu. 2007. Myeloperoxidase inactivates TIMP-1 by oxidizing its N-terminal cysteine residue: an oxidative mechanism for regulating proteolysis during inflammation. *J. Biol. Chem.* 282: 31826–31834.
34. Marcinkiewicz, J., B. M. Chain, E. Olszowska, S. Olszowski, and J. M. Zgliczyński. 1991. Enhancement of immunogenic properties of ovalbumin as a result of its chlorination. *Int. J. Biochem.* 23: 1393–1395.
35. Marcinkiewicz, J., E. Olszowska, S. Olszowski, and J. M. Zgliczynski. 1992. Enhancement of trinitrophenyl-specific humoral response to TNP proteins as the result of carrier chlorination. *Immunology* 76: 385–388.
36. Panizzi, P., M. Nahrendorf, M. Wildgruber, P. Waterman, J. L. Figueiredo, E. Aikawa, J. McCarthy, R. Weissleder, and S. A. Hilderbrand. 2009. Oxazine conjugated nanoparticle detects in vivo hypochlorous acid and peroxynitrite generation. *J.Am.Chem.Soc.* 131: 15739-15744.
37. Chapman, A. L., M. B. Hampton, R. Senthilmohan, C. C. Winterbourn, and A. J. Kettle. 2002. Chlorination of bacterial and neutrophil proteins during phagocytosis and killing of *Staphylococcus aureus*. *J. Biol. Chem.* 277: 9757–9762.
38. Schwartz, J., K. G. Leidal, J. K. Femling, J. P. Weiss, and W. M. Nauseef. 2009. Neutrophil bleaching of GFP-expressing staphylococci: probing the intraphagosomal fate of individual bacteria. *J. Immunol.* 183: 2632–2641.
39. Zheng, L., B. Nukuna, M. L. Brennan, M. Sun, M. Goormastic, M. Settle, D. Schmitt, X. Fu, L. Thomson, P. L. Fox, et al. 2004. Apolipoprotein A-I is a selective target for myeloperoxidase-catalyzed oxidation and functional impairment in subjects with cardiovascular disease. *J. Clin. Invest.* 114: 529–541.
40. Hosken, N. A., K. Shibuya, A. W. Heath, K. M. Murphy, and A. O'Garra. 1995. The effect of antigen dose on $CD4^+$ T helper cell phenotype development in a T cell receptor-αβ-transgenic model. *J. Exp. Med.* 182: 1579–1584.
41. Khor, H. K., M. T. Fisher, and C. Schöneich. 2004. Potential role of methionine sulfoxide in the inactivation of the chaperone GroEL by hypochlorous acid (HOCl) and peroxynitrite ($ONOO^-$). *J. Biol. Chem.* 279: 19486–19493.
42. Shao, B., A. Belaaouaj, C. L. Verlinde, X. Fu, and J. W. Heinecke. 2005. Methionine sulfoxide and proteolytic cleavage contribute to the inactivation of cathepsin G by hypochlorous acid: an oxidative mechanism for regulation of serine proteinases by myeloperoxidase. *J. Biol. Chem.* 280: 29311–29321.
43. Hawkins, C. L., D. I. Pattison, N. R. Stanley, and M. J. Davies. 2008. Tryptophan residues are targets in hypothiocyanous acid-mediated protein oxidation. *Biochem. J.* 416: 441–452.
44. Hawkins, C. L., and M. J. Davies. 1999. Hypochlorite-induced oxidation of proteins in plasma: formation of chloramines and nitrogen-centred radicals and their role in protein fragmentation. *Biochem. J.* 340: 539–548.
45. Rees, M. D., C. L. Hawkins, and M. J. Davies. 2003. Hypochlorite-mediated fragmentation of hyaluronan, chondroitin sulfates, and related *N*-acetyl glycosamines: evidence for chloramide intermediates, free radical transfer reactions, and site-specific fragmentation. *J. Am. Chem. Soc.* 125: 13719–13733.
46. Chiang, C. L., J. A. Ledermann, A. N. Rad, D. R. Katz, and B. M. Chain. 2006. Hypochlorous acid enhances immunogenicity and uptake of allogeneic ovarian tumor cells by dendritic cells to cross-prime tumor-specific T cells. *Cancer Immunol. Immunother.* 55: 1384–1395.
47. Delamarre, L., R. Couture, I. Mellman, and E. S. Trombetta. 2006. Enhancing immunogenicity by limiting susceptibility to lysosomal proteolysis. *J. Exp. Med.* 203: 2049–2055.
48. Chiang, C. L., J. A. Ledermann, E. Aitkens, E. Benjamin, D. R. Katz, and B. M. Chain. 2008. Oxidation of ovarian epithelial cancer cells by hypochlorous acid enhances immunogenicity and stimulates T cells that recognize autologous primary tumor. *Clin. Cancer Res.* 14: 4898–4907.